Your thesaurus codes are:
08.02.1 – 08.14.2 – 13.25.5 – 08.09.2

ASTROPHYSICS
21.11.1997

The X–ray emission of the polar BL Hydri

G. Matt[1], R. Barcaroli[1], T. Belloni[2], K. Beuermann[3], J.M. Bonnet–Bidaud[4], D. De Martino[5], C. Done[6], B.T. Gänsicke[3], M. Guainazzi[7], M. Mouchet[8,9], and K. Mukai[10]

[1] Dipartimento di Fisica, Università degli studi "Roma Tre", Via della Vasca Navale 84, I–00146 Roma, Italy
[2] Astronomical Institute "Anton Pannekoek", University of Amsterdam and Center for High-Energy Astrophysics, Kruislaan 403, NL-1098 SJ Amsterdam, The Netherlands
[3] Universitätssternwarte Göttingen, Geismarlandstrasse 11, D-37083 Göttingen, Germany
[4] CEA, DSN/DAPNIA/Service d'Astrophysique, CEN Saclay, F-91191 Gif sur Yvette Cedex, France
[5] Osservatorio Astronomico di Capodimonte, Via Moiariello 16, I-80131 Napoli, Italy
[6] Department of Physics, University of Durham, South Road, Durham DH1 3LE, U.K.
[7] SAX/SDC Nuova Telespazio, Via Corcolle 19, I–00131 Roma, Italy
[8] DAEC, Observatoire de Paris, Section de Meudon, F-92195 Meudon Cedex, France
[9] Université Denis Diderot, 2 Place Jussieu, F-75005 Paris, France
[10] NASA/GSFC, Code 668, Greenbelt MD 20771, USA

Received / Accepted

Abstract. We report on the analysis of the ASCA and BeppoSAX X–ray observations of the polar system BL Hyi, performed in October 94 and September 96, respectively.

Emission from both poles is apparent from the folded light curves of both observations; the emission from the second pole varies from cycle to cycle, indicating non–stationary accretion there.

The temperature of the post–shock region is estimated to be about 10 keV. Inclusion of both complex absorption and Compton reflection significantly improves the quality of the fit. No soft X–ray component is observed; the BeppoSAX/LECS upper limit to the soft component is in agreement with theoretical expectations for this low magnetic field system.

Key words: Stars: binaries: close – Stars: cataclysmic variables – X–rays: stars – Stars: individual: BL Hydri

1. Introduction

Polar systems, a subgroup of magnetic Cataclysmic Variables (mCVs), contain a highly magnetized white dwarf with polar field strengths ranging from $\sim$ 10 MG $\sim$ to 230 MG (see Beuermann 1997 and references therein), and accreting material from a late type main sequence star. The magnetic field of the white dwarf is strong enough to phase–lock its rotation with the orbital period. These systems are strong X-ray emitters in both soft and hard X-ray bands (see review by Cropper 1990). While hard X-rays are emitted from a standing shock above the white dwarf surface, soft X-rays originate from hot photospheric regions heated either by irradiation from the post-shock plasma (Lamb & Masters 1979) or by dense plasma blobs carrying their kinetic energy deep into the atmosphere (Kuipers & Pringle 1982). Only recently it has been realized that irradiation is important primarily for flow rates sufficiently low for the shock to stand high and heat a large region to UV rather than soft X-ray temperatures (Gänsicke et al. 1995). The "blobby" accretion mode is increasingly important at higher field strengths, because the blobs become more and more compressed when arriving at the surface of the white dwarf (e.g. Beuermann & Burwitz 1995; King 1995 and references therein).

While the soft X–ray component is in general adequately fitted by a black–body spectrum with a temperature of a few tens of eV, it has recently become clear that a simple thermal plasma model is not adequate in reproducing the hard X–ray component of Polars. Reflection from the white dwarf surface, complex absorption and multi–temperature emission may contribute significantly to the spectrum above a few tenth of keV (e.g. Cropper et al. 1997 and references therein).

X–ray emission from the polar system BL Hyi (H01319-68) was first detected by HEAO-1/A-2, and later on by Einstein (Agrawal et al. 1983), EXOSAT (Beuermann & Schwope 1989, hereafter B&S89) and ROSAT (Ramsay et al. 1996; Schwope et al. 1997). In particular, the HEAO-1 and EXOSAT observations showed that copious soft X-ray emission originates from the secondary pole in states of high accretion rate, while the EXOSAT observations showed this pole to become increasingly in-

Table 1. ASCA and BeppoSAX observations log

Instrument	En. range (keV)	Date of obs.	Exp. Time[a] (ks)	Count rate (cts/s)	2-10 keV flux[b] (erg/s/cm^2)
ASCA/GIS2	0.8-10	Oct 11-12, 94	43	0.13	8.0×10^{-12}
ASCA/GIS3	0.8-10	Oct 11-12, 94	43	0.16	
ASCA/SIS0	0.5-10	Oct 11-12, 94	42	0.21	
ASCA/SIS1	0.5-10	Oct 11-12, 94	41	0.16	
BeppoSAX/LECS	0.1-10	Sep 27, 96	3.7	0.02	
BeppoSAX/MECS	1.5-10	Sep 27, 96	12.5	0.12	6.8×10^{-12}

[a] after applying the selection criteria
[b] single–temperature plasma model

active at lower accretion rates. This suggests a picture in which the source switches from one– to two–pole accretion in going from low to high states (B&S89). Recent EUVE observations indicate that the soft X–ray emission is best reproduced by a 17 eV blackbody (Szkody et al. 1997).

Despite all the above observations, the hard X–ray spectrum of BL Hyi was still poorly known before the launch of ASCA and BeppoSAX satellites. ASCA observed this source in October 1994, while BeppoSAX in September 1996, in the context of a Core Program devoted to study flux and spectral variability of Polars on different timescales and on a wide energy range.

In this paper we present temporal and spectral analysis of both ASCA and BeppoSAX observations. Sec. 2 describes the observations and data reduction, while in Sec. 3 and Sec. 4 we present temporal and spectral results, respectively, which are then summarized and discussed in Sec. 5.

2. Observations and data reduction

2.1. ASCA

The ASCA satellite (Tanaka et al. 1994) consists of two CCD's (SIS0 and SIS1) and two GSPC's (GIS2 and GIS3). SIS's have a broader energy range (0.5–10 keV) and better spectral resolution ($\sim$150 eV, roughly constant with energy), while GIS's have a narrower band (0.8–10 keV), poorer energy resolution (about 500 eV at 6 keV) but higher sensitivity above a few keV.

The ASCA observation, carried out on October 11-12 1994, was retrieved from the public archive (preliminary results on this observation were presented by Fujimoto & Ishida 1995). The log of the ASCA observation can be found in Table 1. The observation was performed in a mixture of 1-CCD and 2-CCD modes for the SISs. After cleaning, and selecting BRIGHT2 mode for the SISs, the effective exposure time reduced to about 42, 41, 43 and 43 ksec for SIS0, SIS1, GIS2 and GIS3, respectively. Data analysis was performed usign the XANADU and FTOOLS packages available from NASA Goddard HEASARC. Images, light curves and spectra were created using XSELECT. Spectral fitting and temporal analysis were performed with XSPEC and XRONOS, respectively.

GIS and SIS spectra and light curves have been extracted within a circular region of radius equal to 6' (GIS2 and GIS3), 4' (SIS0) and 3' (SIS1) centred on the source.

For the GISs, background levels have been estimated in an annulus centred on the source with inner radius of 6' and outer radius of 12'. For the SISs, the entire chip containing the source was used, after excluding a circle of 4.5' centred on the source.

The adopted response matrices are those released on March 1995 for the GIS, while for the SISs they have been created with the routine SISRMG in the FTOOLS3.6.0 environment, adopting the March 1997 CTI calibration file.

2.2. BeppoSAX

BeppoSAX (see Boella et al. 1997 for an overall description of the mission) carried both Narrow and Wide field instruments. Two Wide Field Cameras point to opposite directions of each other, and perpendicularly to four, co-aligned Narrow Field Instruments: two imaging instruments, the Low Energy Concentrator Spectrometer (LECS) and the Medium Energy Concentrator Spectrometer (MECS); and two collimated high–energy instruments, the Phoswich Detector System (PDS) and the High Pressure Gas Scintillation Proportional Counter (HPGSPC).

The MECS is actually composed of three units, working in the 1–10 keV energy range, with a total effective area of $\sim$150 cm^2 at 6 keV. The energy resolution is $\sim$8% and the angular resolution is $\sim$0.7 arcmin (FWHM) at 6 keV. The LECS has characteristics similar to that of a single MECS unit in the overlapping band, but its energy band extends down to 0.1 keV.

The effective exposure time for the MECS was 12.5 ksec, but unfortunately, due to instrument problems, only 3.7 ksec of LECS data were collected. The source was not detected by the HPGSPC and the PDS. The log of the BeppoSAX observation can be found in Table 1.

MECS and LECS spectra and light curves have been extracted from a 4' radius circle centred on the source; the MECS event files have been added together after equalization of MECS2 and MECS3 data to the MECS1 energy–PI relationship. (In the following, with the name MECS we denote the sum of the three units.) We selected data acquired with an angle, with respect to the Earth limb, higher than 5°. The background subtraction was performed using blank sky spectra extracted from the same region of the detector field of view. The spectra were fitted using the calibration matrices released on September 1997.

3. Results. Light Curves

3.1. ASCA

We first searched for periodicity in both GIS and SIS light curves. A peak, consistent with the optical period (but with a large error), was found; we then used in the analysis the ephemeris of Schwope (private communication to Szkody et al. 1997), even if they may be no longer fully appropriate (Schwope, private communication):

$$T = 2444884.21926 + 0.0789150406E \quad (HJD) \qquad (1)$$

The corresponding folded light curves for the GIS2 and SIS1 are shown in Fig. 1 (first and second panels from the top, respectively). The two curves are rather similar, despite the SIS' broader and softer energy band. Comparing the curves with that of B&S89 (fourth panel), obtained with the EXOSAT–ME (i.e. in a similar energy band) in October 1985, when the source was at a flux level more than a factor 2 lower (see below), a rough agreement is found, but the maximum seems startin at a somewhat earlier phase in the ASCA curves. Whether this difference is due to an intrinsic difference in the accretion pattern or to the ephemeris being no longer entirely appropriate is impossible to say until new, improved ephemeris will be available. During the minimum, the source is at a level much higher than the background, implying significant emission from the second pole.

A hardness ratio analysis was also performed for the SIS in order to search for spectral variations along the period. No significant variations were observed, and in the spectral analysis (see section 4.1) we therefore used phase–averaged spectra.

3.2. BeppoSAX

In Fig. 2 and in the third panel of Fig. 1 we show the MECS total and folded light curves, respectively. The

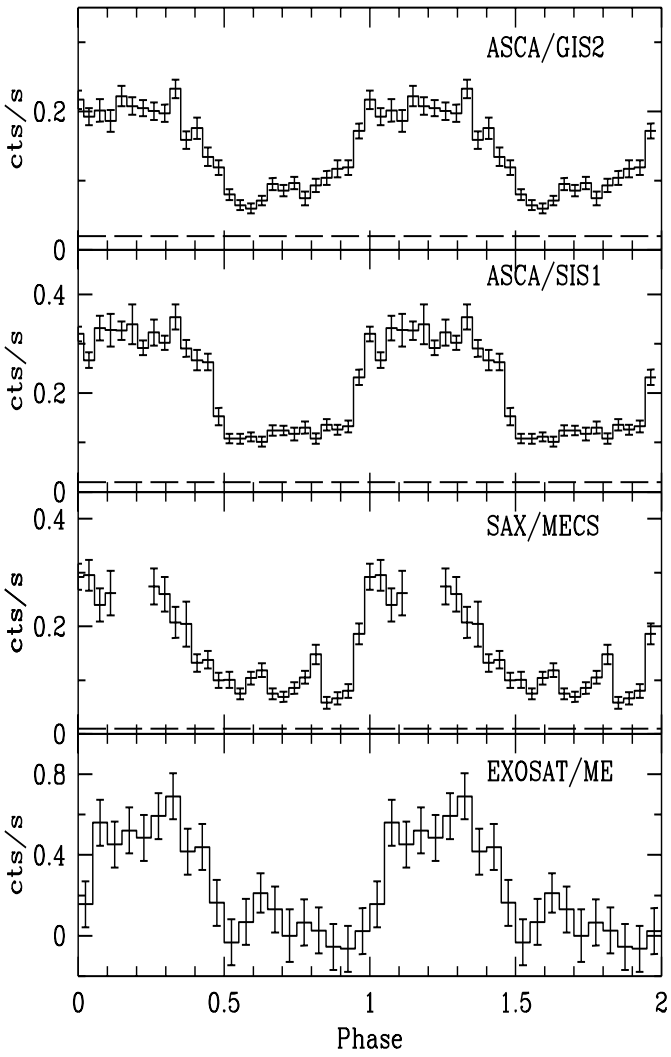

Fig. 1. The light curve of the ASCA/GIS2 (0.8–10 keV) and SIS1 (0.5–10 keV), of the BeppoSAX/MECS (1.5–10 keV) and of the October 1985 observation of the EXOSAT/ME (2–10 keV), from B&S89. The dashed lines in the ASCA and BeppoSAX light curves are the background level. The EXOSAT curve is already background subtracted.

folded light curve is incomplete due to the short observing time. The onset is covered, however, and looks similar to the ASCA light curve.

As in the ASCA light curve, there is significant emission outside the bright phase. It is also important to note that the minimum flux varies drastically between individual orbits (Fig. 2). The BeppoSAX observation spanned about three cycles: in the first and third the level is always well above the background, while in the second cycle the flux drops down to zero and then starts rising, but remaining well below the corresponding level in the other two cycles. The accretion on the second pole is therefore

minimum suggests that it is also inhomogeneous.

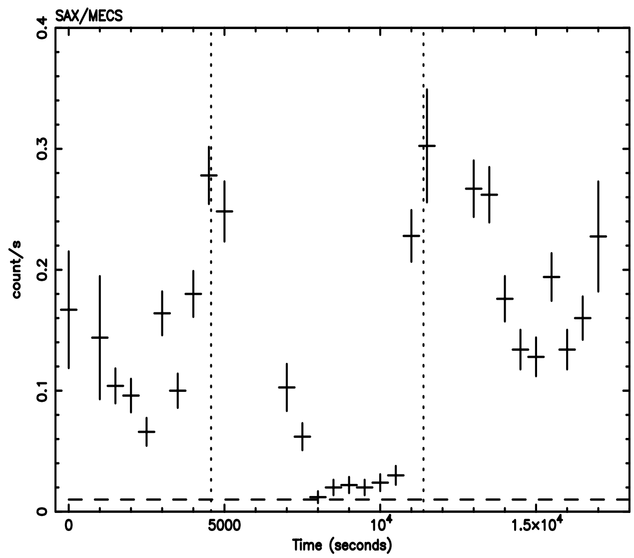

Fig. 2. The light curve of the BeppoSAX/MECS. The dashed horizontal line is the background level. The dotted, vertical lines are separated by the period of the source.

4. Results. Spectra

4.1. ASCA

A hardness ratio analysis was also performed for the SIS in order to search for spectral variations along the period. No significant variations were observed, and in the spectral analysis (see section 4.1) we therefore used phase–averaged spectra.

To perform the spectral analysis, we summed together the two SISs and the two GISs spectra, after having verified that the spectra of the single detectors were consistent with each other. As said above (sec. 3.1), no significant variations of the hardness ratio along the phase is observed (possibly due to the limited statistics in the low phase) and we then used phase–averaged spectra (which are, of course, dominated by the emission at the high phase). The resulting spectra were grouped to have at least 20 counts per bin, in order to apply the χ^2 statistics. As the resulting SIS and GIS spectra were, in the overlapping band, consistent with each other, we fitted them simultaneously to improve the statistical quality of the fits, keeping the two normalizations different to account for possible remaining miscalibration between SIS and GIS. The results of the fits are summarized in Table 2.

The fit with an optically thin isothermal plasma model (i.e. MEKAL model in XSPEC_9.00), even if formally ac-

sentially iron) abundance (model 1 in Table 2). Inspection of the residuals (Fig. 3) indicates the presence of features, probably due to absorption, at low energies (see below). Also, the model does not reproduce adequately the iron line complex. Adding a gaussian line at ~6.7 keV, i.e. from He–like iron, a significant improvement is obtained, with a line EW of about 350 eV: this strongly suggests that the real temperature is lower than estimated by the fit. Furthermore, fitting the spectra in a restricted range with the upper energy fixed to 10 keV and the lower energy increasing from 1 to 6 keV, both the temperature and the abundance monotonically decrease, going from 22 keV and 2.7 to 10.7 keV and 0.7, respectively, again suggesting spectral complexity as the reason for the high temperature found.

To investigate the origin of the observed low energy features in the residuals, we first added a full cold absorber. The quality of the fit increases significantly, and the plasma temperature reduces to ~14 keV, a value more in line with the common value for Polars (e.g. Ishida 1991; Done et al. 1995; Beardmore et al. 1995; Ishida et al. 1997). The fit, however, is still unsatisfactory because the value of the column density, 8×10^{20} cm^{-2}, is largely in excess of that determined by EUVE and ROSAT ($\lesssim 3\times10^{19}$ cm^{-2}: Szkody et al. 1997, Ramsay et al. 1996). We then fitted a partial covering model, in analogy with other sources, in particular Intermediate Polars (Ishida 1991). The fit (model 2) is, from a statistical point of view, somewhat better than that with the full absorber; the absorbing column is about 3×10^{21} cm^{-2}, and the covering factor is ~0.4. Fitting the spectra with more complex absorbers, like that discussed by Done & Magdziarz (1997), does not improve significantly the quality of the fit.

Even if the partial absorber is able to cure the low energy features in the residuals and to significantly reduces the temperature, the abundance remains rather large (about 1.7). Such a high value has never been observed in this type of sources and it will require a very specific evolution of the system. We then investigated whether the high abundance could be an artifact of adopting a single–temperature model instead of a multi–temperature plasma expected since a temperature gradient along the emitting region is obtained from most models (e.g. Aizu 1973; Wu et al. 1994; Woelk & Beuermann 1996). The fit with the CEMEKL multi–temperature model, however, is worse than that with an isothermal plasma and will not be considered further.

We then included in the model the so–called Compton reflection component (Lightman & White 1988; Matt et al. 1991; van Teeseling et al. 1996) in order to account for reflection of the hard radiation by the white dwarf surface. The presence of this component was suggested by Done et al. (1995) and Beardmore et al. (1995) for EF Eri and AM Her, and it is now recognized to be an important ingredient of the X–ray spectrum of magnetic CVs. We adopted

matter to be neutral (van Teeseling et al. 1996) and a mean inclination angle of 60°. As the reflection continuum is expected to go always with the fluorescent iron line at 6.4 keV (e.g. Matt et al. 1991), we added also this feature. As shown in Table 2 (model 3), an improvement in the fit is obtained, and the abundance is now close to one. The best fit value for R (i.e. $F(E) = F_0(E)[1 + RA(E)]$, where F and F_0 denote the total and primary flux, respectively, and $A(E)$ is the albedo of the reflecting matter) is rather high ($\sim$2.5), while a value about unity is expected for 2π illuminated matter; this could be due to the fact that a two–phase plane–parallel geometry is a too simple picture. There is also a mismatch between the amount of reflection continuum and the EW of the 6.4 keV iron fluorescent line: for the latter quantity, a value of about $90(\Delta\Omega/2\pi)$ eV, obtained assuming a $\sim$10 keV illuminating spectrum, solar abundances and a mean observing angle of 60° is in fact expected, to be compared with an observed 90% upper limit of 70 eV. This may suggest the presence in the spectrum of complexities too subtle to be explored with the present data.

We also searched for Sulphur lines at $\sim$2.5 keV; contrary to the claim of Fujimoto & Ishida (1995), based on the very same data, we found no evidence for these lines. Note that the SIS calibration matrices have been quite improved since the time of their analysis, which may explain the difference.

In summary, there is clear evidence for complex absorption: a partial covering model provides an adequate description of the data, even if more complex absorbers cannot be excluded. The continuum is well described by a single temperature plasma model (but, again, multi–temperature components cannot be rejected by the data), but in order to reduce the metal abundance to "normal" values, a reflection component is needed, similarly to the case of other Polars.

4.2. BeppoSAX

The BeppoSAX/MECS spectrum of BL Hyi is shown in Fig. 4. The spectrum is well fitted by a single–temperature thermal plasma model with a temperature of $9.8^{+3.0}_{-1.9}$ keV and solar abundances (χ^2= 52 with 54 d.o.f.). An improvement (χ^2= 46 with 53 d.o.f.) in the quality of the fit is obtained if the metal abundance is left free to vary; the resulting best fit values are: kT=$10.7^{+3.4}_{-2.3}$ keV, A_Z=$1.89^{+0.92}_{-0.62}$. The 2–10 keV averaged flux is about 6.8×10^{-12} erg cm^{-2} s^{-1}. No significant improvements in the fits are obtained with more complex models.

We then used the LECS to estimate the soft X–ray emission, by adding a 17 eV black–body component to the hard one, and assuming a column density of 3×10^{19} cm^{-2} (Szkody et al. 1997). To be conservative, we put the black–body component behind the cold partial screener (model 3 in table 2). The combined LECS+MECS fit gives no black–body flux; the 90% upper limit to this component implies a bolometric soft luminosity less than about 10 times that of the hard one. A much more stringent limit (i.e. $L_{\rm soft} < L_{\rm hard}$) can be put if a 25 eV black–body temperature, as suggested by the ROSAT data (Ramsay et al. 1996), in instead adopted.

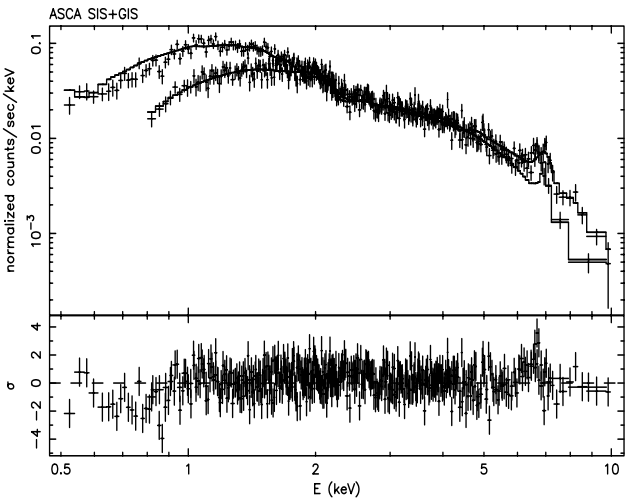

Fig. 3. The ASCA (SIS+GIS) spectrum fitted with an isothermal plasma model (model 1 in Table 2.

5. Discussion

During the ASCA and BeppoSAX observations the source was significantly brighter than during the 'intermediate state' of October 1985, when it was observed by EXOSAT (B&S89). Assuming a 10 keV thermal plasma spectrum, the 2–10 keV phase–averaged flux, estimated with the PIMMS package, was in fact $\sim3\times10^{-12}$ erg cm^{-2} s^{-1} during that EXOSAT observation, while it was $\sim$2.3 and 2.7 times brighter during the BeppoSAX and ASCA observations, respectively. The ASCA flux is instead slightly lower than that measured by Ariel V ($\sim10^{-11}$ erg cm^{-2} s^{-1}, Agrawal et al. 1983).

Comparing both ASCA and BeppoSAX folded light curves with the EXOSAT ones (and in particular with that of October 1985, for which the statistics was the best), one important difference is apparent: there is significant emission from the second pole, while this emission during the EXOSAT observation was less intense, even if still present. As clearly evident from the BeppoSAX light curve, the emission from the second pole is highly variable, changing from cycle to cycle, and then suggesting non–stationary accretion.

The ASCA and BeppoSAX hard X–ray spectra are the first of sufficient quality to reveal spectral complexities. A

Table 2. Best fit parameters for the ASCA (upper panel) ad BeppoSAX/MECS (lower panel) observations. Errors correspond to $\Delta\chi^2$=2.7, i.e. 90% confidence level for one interesting parameter.

#	$N_H{}^a$ (10^{21} cm^{-2})	C^b	kT^c (keV)	$A_Z{}^d$	E.W.^{e} (eV)	R^f (10 keV)	χ^2/d.o.f. (χ^2_r)
1			$31.0^{+7.1}_{-6.5}$	$2.86^{+0.80}_{-0.67}$			704/718 (0.98)
2	$3.2^{+2.4}_{-1.8}$	$0.39^{+0.20}_{-0.08}$	$12.3^{+1.4}_{-1.5}$	$1.76^{+0.19}_{-0.20}$			624/716 (0.87)
3	$2.8^{+3.4}_{-1.8}$	$0.37^{+0.32}_{-0.12}$	$10.1^{+1.9}_{-1.9}$	$0.96^{+0.40}_{-0.31}$	20^{+50}_{-20}	$2.5^{+1.0}_{-1.1}$	609/714 (0.85)
1			$10.7^{+3.4}_{-2.3}$	$1.89^{+0.92}_{-0.62}$			46/53 (0.87)

[a] Column density of the absorber.
[b] Covering fraction of the absorber.
[c] Plasma temperature.
[d] Metal abundance in units of the cosmic value (Anders & Grevesse 1989).
[e] Equivalent width of the 6.4 keV fluorescent iron line.
[f] Relative normalization of the reflection component (see text).

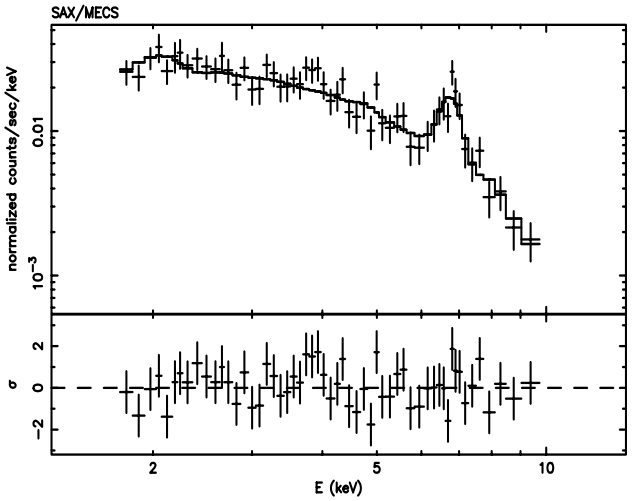

Fig. 4. The BeppoSAX/MECS spectrum fitted with a thermal plasma model.

simple thermal plasma model, even if formally acceptable, should be rejected due to both the presence of features (mostly at the lowest energies) in the residuals and the high temperature and metal (mainly iron) abundance obtained. The inclusion of complex absorption is necessary to cure the low energy features. A partial covering model, with a column density of about 3×10^{21} cm^{-2} and a covering fraction of $\sim$0.4 provides an acceptable description of the spectrum.

The presence of a substantial absorber in front of the hard X-ray component is an important result. It is conceivable that this material is, in fact, the free-falling matter feeding the accretion spot. E.g. in V834 Cen, this material was identified by its Zeeman component shifted in wavelength as expected from the free-fall velocity (Schwope & Beuermann 1990). As the hard X-ray emitting post-shock plasma is probably located in front of the soft X-ray emitting sections of the photosphere, this absorbing material should affect the soft component as well. Due to substantial pre-ionization, however, it may be partially transparent to soft X-rays. On the other hand, the fact that Zeeman absorption from this material was seen in V834 Cen indicates that in that system neutral material is also present. Hence, the soft component may not emerge unhindered and its spectral properties may carry the signatures of the intervening absorber as well as those of the emitter. This must be taken into account when estimating the intensity of the soft component, which was then evaluated (exploiting the sensitivity of BeppoSAX down to 0.1 keV), in the assumption of a partial and neutral absorber in front of the black–body component identical to that covering the hard X–rays emitting region. The upper limit to the soft component luminosity is about ten times that of the hard luminosity, if a black–body temperature of 17 eV (Szkody et al. 1997) is assumed; if, instead, a temperature of 25 eV (Ramsay et al. 1995) is adopted the upper limit is much more tight, reducing to about the hard luminosity. We also computed the upper limit to the black–body to hot plasma flux ratio in the 0.1–2.4 keV, to make comparison with the theoretical expectation (see Fig. 8 in Beuermann 1997). The limits are 5 and 1.3 for the adopted black–body temperatures, consistent with the

systems (Beuermann & Schwope 1994). This is especially true if the field strength of 12 MG measured by Schwope et al. (1995) is characteristic of the main accreting pole. However, also the field strength of 23 MG reported by Ferrario et al. (1996) would still qualify BL Hyi as a low-field system, characterized by a strong hard X-ray component. Only at still higher field strengths is bremsstrahlung effectively suppressed by increasing cyclotron cooling (Woelk & Beuermann 1996, see also Beuermann 1997).

Finally, the inclusion in the spectral model of the reflection component from the white dwarf surface provides a significant improvement in the statistical quality of the fit and reduces the abundance to roughly the solar value. This component has been already detected in a number of Polars (e.g. Done et al. 1995; Beardmore et al. 1995; Ishida et al. 1997; Cropper et al. 1997; Done & Magdziarz 1997) and is now recognized as an important ingredient of their X–ray spectrum. With all these components included, the best fit post–shock temperature results to be about 10 keV (with about 20% uncertainty) in both observations, consistent with the EXOSAT results (B&S89) for the same source and with the values usually found in Polars.

Acknowledgements. We acknowledge the BeppoSAX SDC team for providing pre–processed event files and for their constant support in data reduction. We thank A. Schwope for providing the EXOSAT light curves and for useful discussions. GM acknowledges financial support from ASI, CD from a PPARC AF.

References

Agrawal P.C., Riegler G.R., Rao A. R., 1983, Nat, 301, 318
Aizu K., 1973, Prog. Theor. Phys., 49, 1184
Anders E., Grevesse N., 1989, Geochim. and Cosmochim. Acta, 53, 197
Beardmore A.P., Done C., Osborne J.P., Ishida M., 1995, MNRAS, 272, 749
Beuermann K., 1997, in *Perspectives in High Energy Astronomy and Astrophysics*, in press
Beuermann K., Burwitz V., 1995, in *Cape Workshop on Magnetic Cataclysmic Variables*, eds. D.A.H. Buckley & B. Warner, ASP Conf. Ser., 85, p. 99.
Beuermann K., Schwope A.D., 1989, A&A, 223, 179 (B&S89)
Beuermann K., Schwope A.D., 1994, in *Interacting Binary Stars*, ASP Conf. Ser., 56, 119
Boella G., Butler R.C., Perola G.C., et al., 1997, A&AS, 112, 299
Cropper M., 1990, Space Science Rev., 54, 195
Cropper M., Ramsay G., Wu K., 1997, MNRAS, in press
Done C., Magdziarz P., 1997, MNRAS, submitted
Done C., Osborne J.P., Beardmore A.P., 1995, MNRAS, 276, 483
Ferrario L., Bailey J., Wickramasinghe D.T., 1996, MNRAS, 282, 218
Gänsicke B.T., Beuermann K., de Martino D. 1995, A&A, 303 127
King A. R., 1995, in *Cape Workshop on Magnetic Cataclysmic Variables*, eds. D.A.H. Buckley & B. Warner, ASP Conf. Ser. 85, p. 21.
Kuipers J., Pringle J.E. 1982, A&A, 114, L4
Ishida M., 1991, Ph.D thesis, University of Tokyo
Ishida M., Matsuzaki K., Fujimoto R., Mukai K., Osborne J.P., 1997, MNRAS, 287, 651
Lamb D.Q., Masters A.R. 1979, ApJ, 234, L117
Lightman A.P, White T.R. 1988, ApJ, 335, 57
Matt G., Perola G.C., Piro L. 1991, A&A, 245, 25
Ramsay G., Cropper M., Mason K.O., 1996, MNRAS, 278, 285
Schwope A.D., Beuermann K., 1989, A&A, 222, 132
Schwope A.D., Beuermann K. 1990, A&A 238, 173
Schwope A.D., Beuermann K., Jordan S., 1995, A&A, 301, 447
Schwope A.D. et al. 1997, Proc. 13th North American Workshop on Cataclysmic Variables, ed. S. Howell, in press
Szkody P., Vennes S., Sion E.M., Long K.S., Howell S.B., 1997, ApJ, 487, 916
Tanaka Y., Inoue H, Holt S.S. 1994, PASJ, 46, L37
van Teeseling A., Kaastra J. S., Heise J., 1996, A&A, 312, 186
Woelk U., Beuermann K., 1996, A&A, 306, 232
Wu K., Chanmugam G., Shaviv S, 1994, ApJ, 426, 664

This article was processed by the author using Springer-Verlag LaTeX A&A style file *L-AA* version 3.